

# Low-Threshold InGaAsP Ring Lasers Fabricated Using Bi-Level Dry Etching

Giora Griffel, Joseph H. Abeles, Raymond J. Menna, Alan M. Braun, John C. Connolly, and Marvin King

**Abstract**—We report a novel bi-level etching technique that permits the use of standard photolithography for coupling to deeply etched ring resonator structures. The technique is employed to demonstrate InGaAsP laterally coupled racetrack ring resonators laser with record low threshold currents of 66 mA. The racetrack laser have curved sections of 150- $\mu\text{m}$  radius with negligible bending loss. The lasers operate continuous-wave single mode up to nearly twice threshold with a 26-dB side-mode-suppression ratio. Bi-level etching is of interest for fabrication of mesoscopic or microcavity photonic resonator structures without relying on submicrometer processing.

## I. INTRODUCTION

EVANESCENTLY coupled semiconductor racetrack ring resonators ( $R^3$ s) offer several interesting features for applications such as dense wavelength division multiplexing and RF photonics. Lacking reflectors, their fabrication is free of lapping, cleaving, facet etching and coating, or of concerns arising from high mirror power density. Their spectral characteristics can be determined by photolithography, and single wavelength operation can be achieved without gratings. When combined with other components small ( $<200 \mu\text{m}$ ), low-loss passive and active ring resonators will enable the fabrication of sophisticated photonic integrated circuits that take full advantage of two-dimensional (2-D) chip layouts. Ultimately, with the development of robust and manufacturable fabrication methods, such photonic circuits may include composite linking and switching systems, local oscillator distribution, and true-time delay signal distribution at wavelengths of 1.3 and 1.55  $\mu\text{m}$ .

Previous efforts have been carried out to demonstrate  $R^3$  lasers ( $R^3$ Ls) in both AlGaAs and InGaAsP material systems and using different coupling schemes [1]–[7]. Conventional ridge-waveguide (RWG) circular structures are limited to large diameters ( $\geq 300 \mu\text{m}$ ) due to excessive bending loss. The low index difference of RWG structures causes a significant evanescent portion of the guided mode, which cannot propagate at group velocities exceeding  $c/n_{\text{eff}}$ , to radiate.  $c$  is the speed of light in vacuum and  $n_{\text{eff}}$  the effective refractive index of the mode. Even for large-diameter shallow-etched structures, significant bending loss was evidenced by large threshold currents ranging from 106 to 150 mA [4], [5]. Coupling into deeply etched laser structures was achieved by using either

Y-junction or multimode interference (MMI) couplers. In spite of the reduced bending loss, deeply etched  $R^3$ Ls demonstrated large threshold current values, in excess of 170 mA [6]. Vertical walls etched through the epitaxial waveguide have also been used in small diameter ( $\leq 10 \mu\text{m}$ ) passive ring structures to allow negligible waveguide bending and scattering loss [8], [9]. However, strong confinement caused by deep etching requires submicrometer lateral separation between the ring and coupled waveguides to achieve adequate coupling and requires fabrication tolerances of  $-0.01/+0.02 \mu\text{m}$  [10]. Furthermore, as shown below, when used as a highly transmissive filter, coupling coefficients in and out of the ring resonator must be nearly identical, tightening fabrication constraints even further. Reliance on submicrometer features and tolerances entails significant impediments to achieving a robust manufacturable technology that lends itself to large-scale integration and mass production of ring resonator based photonic circuits.

In this letter, we present an alternative design for ring resonator coupling that uses standard photolithography and that permits excellent control over coupling strength. We employ an InGaAsP ring resonator waveguide in the form of a racetrack laser placed between two straight input/output waveguides as shown in Fig. 1(a). Such a configuration was proposed and analyzed recently for photonics switching and signal processing [11]. In the racetrack configuration presented here, deep etching is needed to reduce bending loss at the curved sections, but is avoided at the gap between the straight sections of the racetrack and the input/output waveguides, where it interferes with coupling. There, a shallower etch which defines the coupling region is halted before removing the epitaxial waveguiding layers [Fig. 1 (b)]. The bi-level etching technique is essentially a modification of the MMI method that provides better control of the coupling in deeply etched structures where, due to the large index contrast, a very large number of modes participate in the interaction. It is important to note that although a straight section of the deeply etched waveguide can support higher-order lateral modes, the curved sections of the racetrack, whose first-order lateral mode cutoff radius is 250  $\mu\text{m}$ , discriminate in favor of single lateral mode operation [6].

It is apparent that the issues of coupling strength and coupling efficiency are of utmost importance to the performance of  $R^3$ Ls. They not only affect power extraction efficiency, but introduce intracavity loss that increases the threshold current. We consider the electromagnetic field transmitted from the input to the output coupling waveguide of Fig. 1(a) through the resonator, as given by

$$\frac{E_o}{E_i} = \frac{t_1 t_2 \exp[-i(\beta_a L_a + 2\beta_c L_c)]}{1 - r_1 r_2 \exp[-i 2(\beta_a L_a + 2\beta_c L_c)]} \quad (1)$$

Manuscript received July 27, 1999; revised October 15, 1999. This work was supported in part by the Air Force Rome Labs under Grant SBIR F-30602-97 and in part by the National Institutes of Health (NSF) under Grant ECS-9634617.

G. Griffel, J. H. Abeles, R. J. Menna, A. M. Braun, and J. C. Connolly are with the Sarnoff Corporation, Princeton, NJ 08543-5300 USA.

M. King is with the Riverside Research Institute, New York, NY 10036 USA.

Publisher Item Identifier S 1041-1135(00)01096-X.

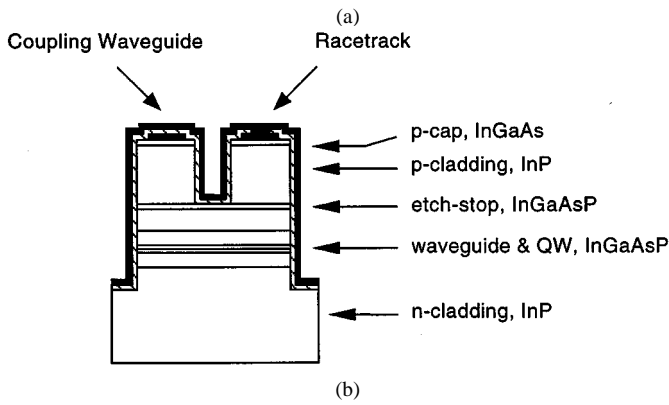
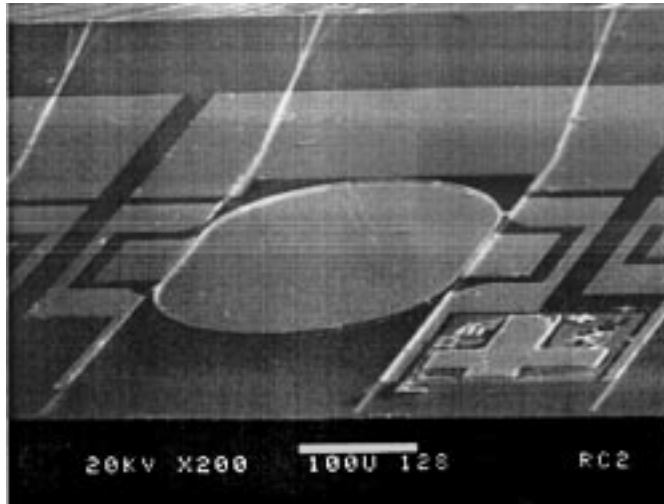


Fig. 1. (a) Scanning electron micrograph of the racetrack laser. (b) Schematic cross-sectional diagram taken at the coupling region between the ring and one of the straight waveguide showing the shallow- and the deep-etched regions.

where  $t_{1,2}$  are the coupling coefficients of the upper and lower coupling regions, and  $\beta_{a,c}$  are the propagation constants in the curved sections and in the straight section of the racetrack, respectively.  $L_a$  is the total length of the curved sections,  $2\pi a$ ,  $a$  being the radius of the ring, and  $L_c$  the length of each straight section.  $r_{1,2}$  represent the fraction of incident field which is *not* transmitted from one waveguide to the other in the coupling region, where it can be shown, using the coupled-mode formalism and power conservation, that  $|r_{1,2}|^2 + |t_{1,2}|^2 = 1$ . This transmission function, (1), reveals that a ring resonator is analogous to a Fabry–Perot (FP) resonator. That is, at zero gain, the spectrum is characterized by Lorentzian-like transmission peaks at resonance with free spectral range (FSR) of  $c/(n_{\text{eff}}^a L_a + 2n_{\text{eff}}^c L_c)$ . The couplers play a role analogous to FP mirrors. To obtain unity transmission at resonance with zero gain the coupling coefficients should be equal, i.e.,  $t_1 = t_2$ , which for the case of deeply etched structure predicates extremely tight fabrication constraints.

Our OMCVD-grown epilayer structure includes three compressively strained InGaAsP quantum wells imbedded in a 70-nm waveguide structure of two compositions with bandgap energy  $E_g = 1.13$  and 1.00 eV. Cladding layers are InP. The fabrication involves several steps not normally used in conjunction with conventional RWG laser processing. These include: 1) liftoff metal deposition of closely spaced lines and

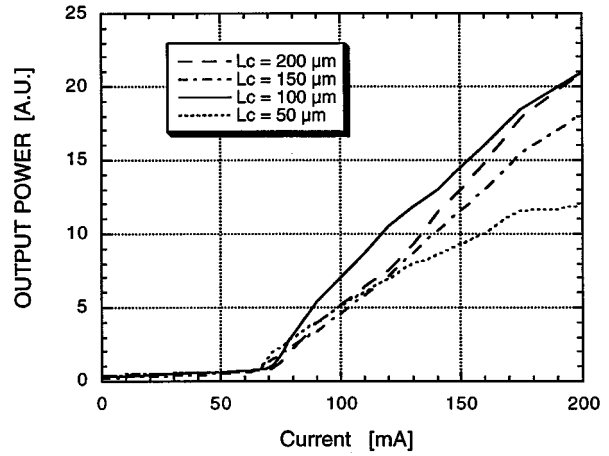


Fig. 2. Output power characteristic of racetrack lasers with coupling lengths ranging from 50 to 200  $\mu\text{m}$ , showing nearly the same threshold current for all configurations with improved differential efficiency for 100- $\mu\text{m}$  coupler.

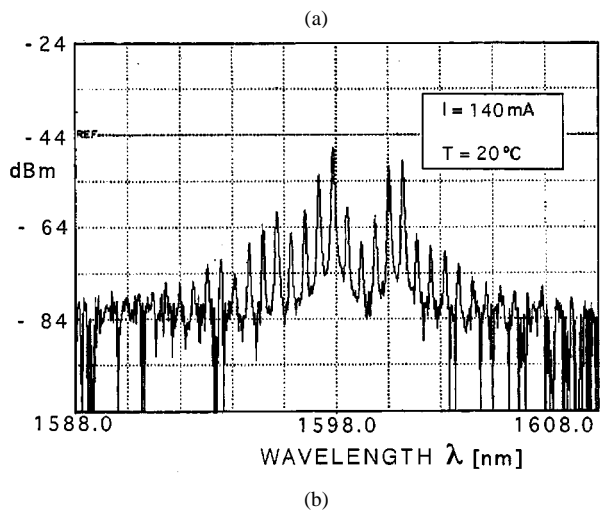
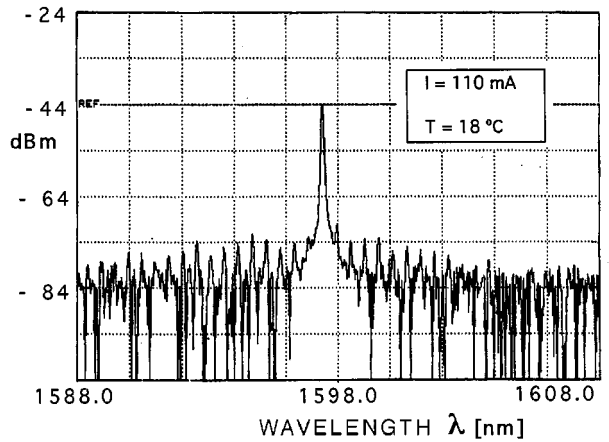


Fig. 3. (a) Lasing spectra of the racetrack laser at drive current  $I = 110$  mA, showing single mode operation with SMSR = 26 dB. Single longitudinal mode operation is maintained up to nearly twice  $I_{\text{th}}$  and (b) lasing spectra at  $I = 140$  mA showing nonlinear change to a broad spectrum.

2) both shallow and deep etching with no feature undercutting. For the coupling channel between parallel waveguides [cross section in Fig. 1(b)] an asymmetric structure is fabricated. The waveguiding geometry is first defined by  $\text{H}_2/\text{CH}_4$  reactive

ion etching, timed to remove the p-type cladding layer and reveal the upper surface of the waveguide structure. Next, the coupling region is coated with a second dielectric layer. Smooth sidewalls extending through the waveguide structure are etched, except in the coupling region protected by the second dielectric layer.

A bend radius of 150  $\mu\text{m}$  is combined with four different coupler lengths of 50, 100, 150, and 200  $\mu\text{m}$ , positioned at the center of the straight section of the racetrack, which is 50  $\mu\text{m}$  longer. The width of ridges throughout the structure is 2.5  $\mu\text{m}$  and the gap between resonator and coupling waveguides is 2  $\mu\text{m}$ . The coupling waveguides, which extend beyond the racetrack ring resonator, are cleaved, and output facets optically coated to  $\approx 3\%$  reflectivity. Fig. 1(a) is a scanning electron microscope (SEM) image showing the racetrack resonator and the straight coupling waveguides. Biasing electrodes are provided separately for the ring resonator and the portion of each of the two coupling waveguides extending from the resonator to the autoregressive-coated facet. The latter are biased approximately to transparency to facilitate laser characterization. The remaining portion of the coupling waveguides extending toward the rear facet are bent and flared to cut down the effective reflectivity from the unused facet. These sections can be also reverse-biased to further reduce parasitic reflectivity.

Continuous-wave (CW) room-temperature relative  $L$ - $I$  characteristics of devices having all four  $L_c$  values are shown in Fig. 2. These indicate threshold currents varying from 66 mA for the 50 and 150  $\mu\text{m}$  coupling region devices to 72 mA for the 100 and 200  $\mu\text{m}$  devices. These threshold currents are more than a factor of two lower than the lowest-threshold InP ring lasers reported in the literature [6]. We believe that this dramatically improved threshold performance is attributable to our bi-level etched R<sup>3</sup>L design. The corresponding threshold current densities range between 2.145  $\text{kA}/\text{cm}^2$  for the 200- $\mu\text{m}$  coupler to 2.53  $\text{kA}/\text{cm}^2$  for the 50- $\mu\text{m}$  coupler. These values are within a factor of two to three of threshold current densities of world-record RWG FP lasers with similar dimensions and fabricated from similar material [12]. Changing the bias level of the straight coupling waveguides has a negligible effect on the threshold current.

The small dependence of the threshold current on the coupling length indicates that the loss in the cavity is governed mostly by mechanisms other than the output coupling, such as scattering due to wall roughness, bending loss, or modal transition from the curved to the straight section and from the deeply etched to the shallow etched transition regions. Passive measurements of the devices were taken at longer wavelength using temperature tuned InGaAsP DFB laser operating at 1.655–1.659  $\mu\text{m}$ . Depth of modulation of about 20% was observed with finesse of 2.5. Coupling efficiency of 20% and effective distributed loss, combining bending, mode matching and scattering loss, of 15.1 [ $\text{cm}^{-1}$ ] were calculated.

The CW spectrum of an R<sup>3</sup>L with 100- $\mu\text{m}$ -long couplers is shown in Fig. 3(a). It exhibits single longitudinal mode

operation with a side-mode suppression ratio better than 26 dB. Many ring laser modes are clearly visible as noise peaks below that level. Single mode lasing is obtained up to nearly twice threshold. As shown in Fig. 3(b), at 140 mA, the spectrum abruptly changes to a broad spectrum of the same ring laser modes, suggestive of passively modelocked self pulsation. The separation of these modes was observed to match and scale inversely with the circumference of the racetrack.

In conclusion, we have demonstrated an InGaAsP racetrack ring resonator laser employing a novel bi-level etched structure, which can be defined by conventional photolithography, that incorporates low-loss curved waveguides and lateral couplers. The lasers exhibit a threshold current of 66 mA, which is the lowest value of any InP ring resonator lasers reported to date. They operate in a single mode to nearly twice the threshold with a 26-dB side-mode suppression ratio. This novel fabrication technique can be also applied to the construction of passive ring resonators devices such as filters, modulators, routers, and detectors.

## REFERENCES

- [1] J. P. Hohimer, D. C. Craft, G. R. Hadley, G. A. Vawter, and M. E. Warren, "Single frequency continuous wave operation of ring resonator diode lasers," *Appl. Phys. Lett.*, vol. 59, no. 26, pp. 3360–3362, 1991.
- [2] J. P. Hohimer and G. A. Vawter, "Unidirectional semiconductor ring lasers with racetrack cavities," *Appl. Phys. Lett.*, vol. 63, pp. 2457–2459, 1993.
- [3] ———, "Passive mode locking of monolithic semiconductor ring lasers at 86 GHz," *Appl. Phys. Lett.*, vol. 63, pp. 1598–1600, 1993.
- [4] T. F. Krauss, R. M. De La Rue, P. J. R. Laybourn, B. Vogel, and C. R. Stanley, "Efficient semiconductor ring lasers made by a simple self-aligned fabrication process," *IEEE J. Select. Topics Quantum Electron.*, vol. 1, pp. 757–761, June 1995.
- [5] T. F. Krauss, R. M. De La Rue, and P. J. R. Laybourn, "Impact of output coupler configuration on operating characteristics of semiconductor ring lasers," *IEEE J. Lightwave Technol.*, vol. 13, pp. 1500–1507, July 1995.
- [6] R. van Rooijen, E. C. M. Pennings, M. J. N. van Stralen, J. M. M. van der Heijden, T. van Dongen, and B. H. Verbeek, "Compact InP-based ring lasers employing multimode interference couplers and combiners," *Appl. Phys. Lett.*, vol. 64, no. 14, pp. 1753–1755, 1994.
- [7] P. B. Hansen, G. Raybon, M. D. Chien, U. Koren, B. I. Miller, J. M. Vierdiell, and C. A. Burrus, "A 1.5- $\mu\text{m}$  monolithic semiconductor ring laser: CW and mode-locked operation," *IEEE Photon. Technol. Lett.*, vol. 4, pp. 411–413, May 1992.
- [8] B. Little, G. S. T. Chu, H. Haus, J. Foresi, and J. P. Laine, "Micro-ring resonator channel dropping filters," *IEEE J. Lightwave Technol.*, vol. 15, p. 998, <month?> 1997.
- [9] D. Rafizadeh, J. P. Zhang, S. C. Hagness, A. Taflove, K. A. Stair, and S. T. Ho, "Nanofabricated waveguide-coupled 1.5  $\mu\text{m}$  microcavity ring and disk resonators with high Q and 21.6-nm free spectral range," in *Proc. CLEO '97*, Postdeadline Paper, pp. CPD23-2–CPD23-3.
- [10] D. Rafizadeh, J. P. Zhang, R. C. Tiberio, and S. T. Ho, "Propagation loss measurements in semiconductor microcavity ring and disk resonators," *IEEE J. Lightwave Technol.*, vol. 16, pp. 1308–1313, July 1998.
- [11] G. Griffel and S. Arnold, "Synthesis of optical filters using meso-optical ring resonator arrays," presented at the IEEE Lasers and Electro Optics Society 10th Annu. Meeting, San Francisco, CA, November 1997.
- [12] J. A. Abeles, R. J. Menna, D. Z. Garbuzov, R. U. Martinelli, D. R. Capewell, A. R. Triano, R. J. Matarese, M. G. Harvey, D. B. Gilbert, L. A. DiMarco, J. C. Connolly, and A. L. Cook, "High power, tunable, narrow linewidth 1.55  $\mu\text{m}$  distributed feedback diode lasers," in *Proc. 1998 Conf. Lasers and Electro-Optics*. Washington, DC, 1998, p. 301.